ELSEVIER

Journal of Photochemistry and Photobiology A: Chemistry 129 (1999) 71–80

Journal of Photochemistry and Photobiology A:Chemistry

www.elsevier.nl/locate/jphotochem

Comparison of the fluorescence behaviour of rhodamine 6G in bulk and thin film tetraethylorthosilicate derived sol–gel matrices

Graham Hungerford [a,*], Klaus Suhling [b], João A. Ferreira [a]

[a] *Dep. Física, Universidade do Minho, 4709 Braga, Portugal*

[b] *Astrophysics Group, Blackett Laboratory, Imperial College of Science, Technology and Medicine, London SW7 2BZ, UK*

Received 3 August 1999; accepted 13 August 1999

Abstract

A comparison has been made between thin film and bulk sol–gel derived matrices produced from the same reaction mixture. This was carried out by the incorporation of various concentrations of rhodamine 6G and monitoring the dyes fluorescence behaviour using both steady state and time-resolved fluorescence spectroscopy. Measurements were performed on matrices, which were considered to be in a stable condition and unlikely to undergo any further major structural changes. In the thin film matrices the fluorescence decay was non-exponential and appeared to relate to different environments for the dye molecules. This was supported by anisotropy measurements that imply that dye is present adsorbed to the silica matrix as well as solvated within some of the pores. In the bulk matrices the time-resolved fluorescence decay was monoexponential (decay time 4.34 ns) and on increasing the rhodamine 6G concentration the main phenomenon observed was that of self-absorption. Evidence was found for the presence of solvent within the bulk matrix and time-resolved fluorescence anisotropy indicated the existence of two main environments of differing viscosity (7 and 195 mPa s), which can relate to different pore sizes. Measurements of energy transfer from rhodamine 6G to malachite green showed a much greater than expected efficiency at low acceptor concentrations. This is attributed to confinement of the dye within the pore and reflects a distribution of pore sizes.

Keywords: Thin film and bulk sol–gel derived matrices; Time-resolved fluorescence; Anisotropy; Energy transfer

1. Introduction

The use of glass matrices produced by the sol–gel technique [1] has increased in a marked manner. There are many factors responsible; for example, the technique is low cost and capable of producing uniform glasses of high purity. The sol–gel technique also has the advantage that the glass matrices are produced at a low processing temperature, typically several tens of degrees Celsius, as opposed to a couple of thousand degrees for a 'normal' glass. This fact allows for the inclusion of fluorescent dyes and other optically active molecules, which could not withstand the higher processing temperatures of standard glass production. It is also possible to produce glasses with a high porosity using this technique. The matrix may be used as a host for active species and can have many applications [2–5]. Utilising the matrix to incorporate and study fluorescent molecules has formed an important area of research, both by using the fluorescent dyes to monitor the sol–gel process [6–8] and also the sol–gel glass as an environment in which to study the photophysics of dye molecules as well as their interaction with the matrix [9–14]. For example, aggregation effects have been seen to reduce during the gelation process [15] and the photostability of some dyes has also been found to become enhanced when incorporated in a sol–gel derived matrix [16,17]. There have been applications, such as solid state lasers [18], sensors [19] and non-linear effects [20]. The use of a sol–gel matrix also offers the opportunity to isolate molecules and to restrict collisional deactivation when studying a relatively high concentration of dye in a solid matrix. This allows the photophysics of concentration effects to be studied while minimising collisional interactions between dye molecules. Hence they can provide suitable matrices for observing aggregation and self-absorption effects [21,22].

Here we attempt to assess the steady state and time-resolved fluorescence behaviour of rhodamine 6G encapsulated in both thin film and bulk monolith sol–gel derived glass matrices at various concentrations. It was hoped to ascertain information regarding differences in dye behaviour

* Corresponding author.
E-mail address: graham@fisica.uminho.pt (G. Hungerford)

1010-6030/99/$ – see front matter
PII: S1010-6030(99)00176-8

as well as to elucidate any structural differences between the two forms of matrix produced from the same chemical reaction mixture. To this end we choose to use acid catalysed tetraethylorthosilicate (TEOS) derived matrices in which to incorporate the dye. The matrix was also probed using rhodamine 6G in conjunction with malachite green to provide information by the measurement of energy transfer by the Förster mechanism. Anisotropy measurements were also performed to provide information concerning the viscosity of the dye's microenvironment. In this work we choose to monitor the final dried matrix at a time when it was considered to be in a stable condition, when minimal structural changes should occur, rather than following the sol–gel process itself. The aim was to produce sol–gel materials, which were stable in air and of good optical quality, to study fluorescent dye behaviour.

2. Experimental details

2.1. Sample preparation

Sol–gel matrices of SiO_2 were prepared under acidic conditions by hydrolysis and condensation of TEOS, from Aldrich, using ethanol (Merck) as solvent with distilled water containing hydrochloric acid (Merck) as the catalyst. The method employed was adapted from Matsui and Usuki [14]. The initial solutions contained variable amounts of the dyes to be studied, which were dissolved in the ethanol. Rhodamine 6G was obtained from Merck and malachite green from DIFCO. All were used without further purification. The gel-formation reactions can be summarised as follows,

$$Si(OC_2H_5) + 4H_2O \rightarrow Si(OH)_4 + 4C_2H_5OH$$

$$nSi(OH)_4 \rightarrow nSiO_2 + 2nH_2O$$

The mole ratio $[H_2O]/[TEOS]$ used was 6 and pH was about 3. Samples were prepared by stirring a mixture of TEOS and ethanol (containing a volume of a stock solution of 10^{-3} M dye in ethanol) to which water acidified with HCl was added. After about an hour of stirring the reaction mixture was transferred to an oven, which was set to 60°C. Thin films were produced by dipping glass slides at a constant speed in the solution during the first stages of the gelation process. This was typically after the samples had spent c.a. 4 h at 60°C. Film thickness was evaluated from the wavelength of interference maxima and minima of the transmission spectra in the region where dye absorption is negligible (above 800 nm). The average thickness was found to be about 1.5 μm. The remaining reaction mixture could then be used to form 'bulk' samples.

The bulk monolith samples (with dimensions of c.a. 15 mm × 5 mm × 5 mm) were formed by using standard 10 mm internal pathlength plastic cuvettes as moulds. These were covered and kept at 60°C for at least 2 weeks. Samples were considered ready when no discernible decrease in volume was observed. By this sample preparation technique, crack-free samples of good optical quality could be obtained.

2.2. Measurements

Absorption spectra were acquired with a Shimadzu UV-3101 and the fluorescence spectra with a SPEX Fluorolog. Steady state intensity mapping of the bulk sol–gel glass sample was performed using an image intensifier operating in the photon counting mode in conjunction with a CCD camera mounted to the camera port of a trans-illumination microscope (Zeiss). This microscope was also equipped with an optical fibre (1 mm diameter) with which to channel the excitation light (500 nm) to the sample. The fluorescence was monitored at 90° via a cut off filter (530 nm) and photon events were recorded with a Pulnix TM-6701AN full frame progressive scan camera. Frames containing the photon events were read into a PC by a DIPIX FPG-44 framegrabber. To avoid overloading the intensifier all measurements were performed in the dark at low light levels.

Fluorescence decays were measured with a time-correlated single-photon counting apparatus equipped with a hydrogen-filled coaxial flashlamp excitation source. The excitation wavelength was chosen either using a monochromator or a 500 nm interference filter (10 nm bandpass). The latter was mainly used for the anisotropy measurements. The fluorescence emission was wavelength selected using Shott glass 550 nm cut-off filter and detected using a Philips XP2020Q photomultiplier. Unless otherwise stated, the measurements were carried out with the emission monitored at 90° to the excitation (i.e. the light path through an average bulk sample would be about 5 mm). In the case of the film samples, the measurement geometry was such that they were measured 'front face' at 45° to the excitation and emission. The instrumental profile was obtained by replacing the sample with a scatterer. The time calibration was about 0.1 ns per channel and decays were measured to 10,000 counts in the peak. The data were analysed using a least squares reconvolution procedure (IBH Consultants). Errors were taken as three standard deviations and the goodness of fit was judged in terms of a χ^2 value and weighted residuals.

3. Results and discussion

3.1. TEOS thin film and bulk matrix characteristics

Prior to the observation of the fluorescence of dyes incorporated into the two forms of sol–gel matrix a study was performed on the matrices devoid of dopants. The NIR absorption spectrum of the thin films displayed interference fringes, while that for the bulk appeared fairly featureless in the region 350–800 nm, see Fig. 1. At wavelengths below

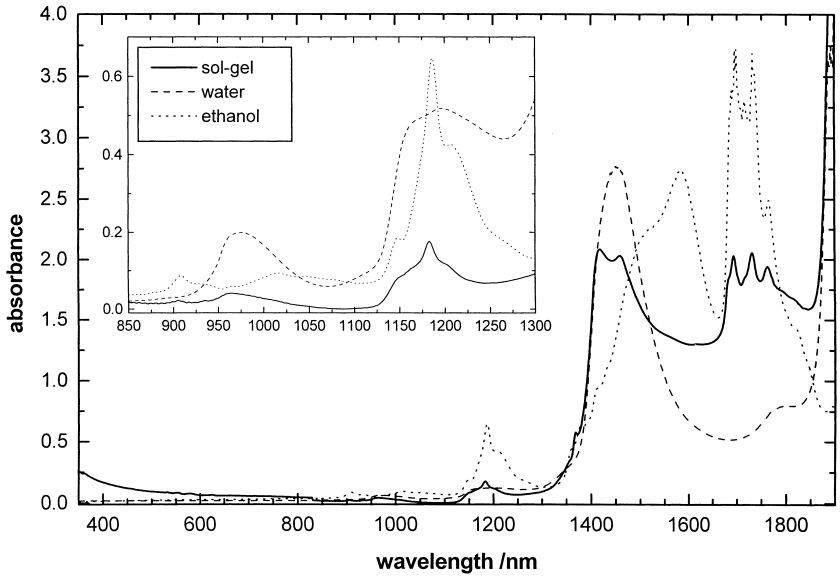

Fig. 1. Comparison of the near infrared absorption spectra of a sol–gel monolith with water and ethanol (the pathlength was 2 mm for the water and 10 mm for the other samples). The inset shows the absorption for these samples, scaled to a 10 mm pathlength, in the region 850–1300 nm.

350 nm there is an increase in absorption and at wavelengths longer than 800 nm several absorption bands could be observed. Of particular interest are the (harmonic) absorption bands, which can be found around 970 and 1180 nm. The former relates to water and the latter to either ethanol or TEOS. With the thin film samples it was not possible to make any judgement because of the thinness of the films (low absorbance) and the fact that the features were obscured by the fringe pattern. In the case of the bulk monoliths, however, the NIR absorption spectra showed that both water and ethanol or unreacted TEOS are still to be found in the 'dried' matrix. This fact was also confirmed using differential scanning calorimetry (DSC), where on scanning from 0 to 300°C the presence of the two solvents was detected. Thermogravometric analysis (TGA) also confirmed this and yielded a value of 20% for the proportion of the weight attributable to solvent. From these measurements it appears that the most likely origin of the band at 1180 nm is ethanol rather than unreacted TEOS. An estimate made from the strength of the absorption bands at 970 and 1180 nm indicated that a monolith could contain of 20% water and 25% ethanol by volume. It is assumed that this is locked in the pores in the interior of the matrix. Some evidence for this has come from anisotropy measurements of rhodamine 6G in TMOS matrices [23].

Although the NIR spectrum for the monolith sample appears dominated by 'free solvent' there are also bands to be seen, which have previously been related to pore water. Literature [1] reviews these and the assignments following are based on this reference. In our spectrum a small peak is observed around 939 nm, which has been assigned to the $3\nu_3 + 2\nu_{OH}$ (a second overtone of 2816.88 nm — a stretching vibration of a Si–O–H bond). Another small, but sharper peak, is seen at 1367 nm ($2\nu_2$), which is an overtone of a hydroxyl stretching vibration. At 1459 nm a band (assigned as an overtone of 2919.7 nm, ν_4) is seen relating to the stretching vibration of adsorbed water. Thus it appears that our bulk sample contains both water bound to the inside of the pore and a large amount of free water and ethanol. Further analysis of bands at longer wavelengths was hampered by the large absorption of the sample.

Table 1
Estimates for the composition of the bulk and thin film samples based on the NIR and density measurements showing the extreme values. For the thin film sample case A relates to a scenario where the film contains a similar fraction of liquid as the bulk and case B when no liquid is present. The values given are volume fractions. Assuming densities of 2.3 gcm^{-3} for silica, 0.79 gcm^{-3} for ethanol and 1 gcm^{-3} for water

Composition	Bulk (%)	Film (%)	
		A	B
Silica	48	17	30
Ethanol	25	25	–
Water	20	20	–
Void	7	38	70

An estimate of the densities of the two types of sample was made and this indicated that on an average the films (assuming a uniform thickness of 1.5 μm) had a density of about 0.7 gcm^{-3} compared with 1.5 gcm^{-3} for a bulk sample. These values are less than that for sintered porous silica gels (2.1–2.3 gcm^{-3}) [1]. Combining the density measurements with the NIR data, assuming densities of 2.3 gcm^{-3} for silica, 0.79 gcm^{-3} for ethanol and 1 gcm^{-3} for water, we obtain the volume fractions presented in Table 1. It should be noted that these estimates are more likely to be the extreme cases. However, for the bulk sample if we take the values presented in Table 1 then the weight fraction of solvent is about 26%. This is close to the value obtained from

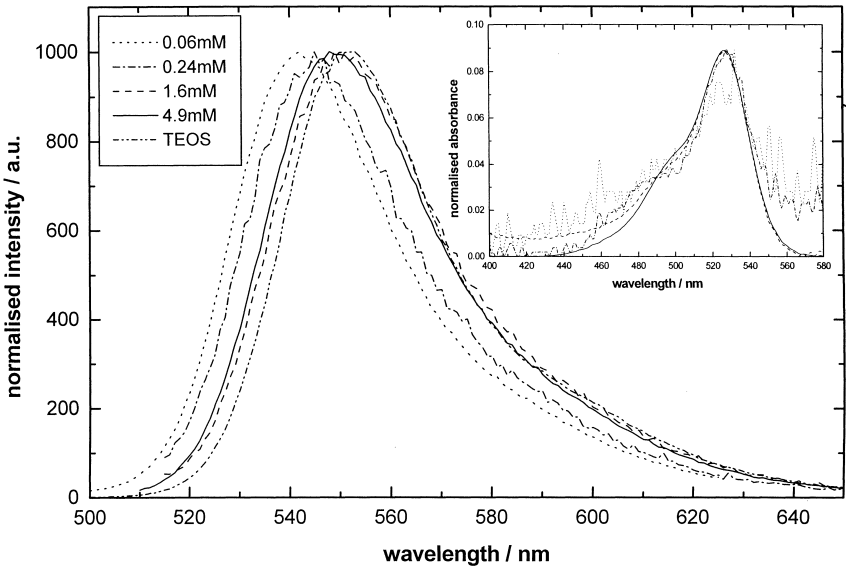

Fig. 2. The steady state fluorescence spectra of different concentrations of rhodamine 6G in thin films formed by the sol–gel technique. The spectrum for the dye in TEOS with ethanol added to aid solubility is shown for comparison. The inset shows the corresponding absorption spectra for the sol–gel films, normalised to the highest concentration. The '*x*-value' refers to the amount (in ml) of 10^{-3} M rhodamine 6G stock solution used in the initial reaction mixture.

the TGA and adds credence to our estimates. The estimates of the composition of the thin film sample are also based on the two limiting cases, (case A) where the film contains a similar fraction of liquid as the bulk and where it contains no liquid (case B). These estimates clearly show that the film sample is more porous than the bulk and contains more voids. However, it should be stressed that these are extreme estimates and it is very unlikely that the films will contain any significant amount of solvent as the drying process is very fast. Therefore, in reality, the composition should be near to that given in case B. Also there is a possibility that if our bulk samples were to be left for even longer periods of time a further reduction in the amount of liquid trapped in the matrix might occur.

3.2. Fluorescence behaviour of rhodamine 6G incorporated in the matrices

3.2.1. Thin film matrices

The steady state fluorescence emission and absorption spectra for the thin film samples containing rhodamine 6G are given in Fig. 2. From the absorption spectra of these samples (Fig. 2 shown as an inset and scaled) there does not appear to be any significant indication of aggregation. The calculated concentrations for each of the samples (for a film thickness of 1.5 μm and a molar extinction coefficient of 82,000 [4]) are 0.06, 0.24, 1.6 and 4.9 mM. These values were found to correlate well to the amount of dye in the initial reaction mixture (concentration (mM) was ca. 0.49 times volume (ml) of 10^{-3} M stock solution used).

The fluorescence spectrum for the film samples (Fig. 2) displays a shift to longer wavelengths with increasing concentration. The origin of the shift has previously been attributed to aggregate formation [9,24] and may even be an artefact of self-absorption. However, because of the geometry used the latter effect should be negligible. The peak emission of the higher concentrations of dye coincide with that for rhodamine 6G in TEOS (a small amount of ethanol, ca. 3% of the total volume, was also added to improve dye solubility), which has a peak emission at 551 nm. This suggests that the origin of the shift is most likely environmental. A greater number of dye molecules having to occupy a more silica-like environment with increasing concentration could explain this effect. For example, after the filling up of 'more favoured' solvated pores, the drier pores start to become filled with the rhodamine 6G, which is adsorbed to the silica.

Time-resolved fluorescence measurements were performed on these films and in all cases the decays were found to be non-exponential. Similar behaviour has been reported for the same dye in TMOS matrices, except at very low concentrations [24], and for a variety of molecules adsorbed to metal oxides [25], however, the reason for this behaviour is still unclear [26]. Analysing the decays as a sum of exponentials allowing the lifetime and pre-exponential parameters to float (Table 2) produces reasonable fits to the data. However, there is no discernible trend and the errors recovered are not insignificant. Calculation of a mean decay time shows an overall decrease in the decay time although the lower concentration data appear hard to interpret. A further attempt at analysis (also presented in Table 2) was then made fixing one decay time at 4.3 ns. This is the value obtained for our bulk samples (see later) and also that reported in wet silica gels [27] and adsorbed to vesicles [28]. In this case good fit to the data are found throughout and

Table 2
Analysis of the time-resolved fluorescence decays for rhodamine 6G in thin film matrices using a biexponential analysis of the form $I(t) = \alpha_1 \exp(-t/\tau_1) + \alpha_2 \exp(-t/\tau_2)$. The mean decay time is given calculated from the analysis with all the parameters floating. The pre-exponential factors are given normalised to 1 and errors as 3 standard deviations

Concentration (mM)	All parameters allowed to float				τ_2 fixed at 4.3 ns		
	Decay time (ns)	Pre-exponential	χ^2	Mean decay time (ns)	Decay time (ns)	Pre-exponential	χ^2
0.06	2.27 ± 0.33	0.48	1.10	3.36	2.08 ± 0.15	0.44	1.07
	4.37 ± 0.21	0.52			4.30	0.56	
0.24	3.37 ± 0.68	0.72	1.13	3.73	3.10 ± 0.19	0.47	1.14
	4.66 ± 0.05	0.28			4.30	0.53	
1.6	1.47 ± 0.65	0.16	1.16	3.36	3.13 ± 0.19	0.68	1.19
	3.72 ± 0.05	0.84			4.30	0.32	
4.9	1.83 ± 0.61	0.61	1.06	2.24	2.20 ± 0.06	0.95	1.08
	2.72 ± 0.89	0.39			4.30	0.05	

Table 3
Datasets given in Table 2 analysed using Förster (3-D) analysis, of the form $I(t) = \alpha_1 \exp[(-t/\tau_1) - 2\gamma(t/\tau_1)^{1/2}] + \alpha_2 \exp(-t/\tau_2)$, where τ is the lifetime and $\gamma = C[(2\pi^{3/2}R_0{}^3N)/3000]$, for two cases. The first with only one species fluorescing and transferring energy and the second with the monomer (decay time fixed at 4.3 ns) fluorescing and transferring energy to a fluorescing dimer (τ_2)

Concentration (mM)	Only monomer fluorescing			Two fluorescing species, τ_1 fixed at 4.3 ns				
	τ (ns)	γ	χ^2	α_1	γ	τ_2 (ns)	α_2	χ^2
0.06	5.06 ± 0.21	0.371	1.06	0.55	–	2.07 ± 0.15	0.45	1.08
0.24	4.18 ± 0.12	0.105	1.17	0.52	–	3.10 ± 0.18	0.48	1.15
1.6	4.00 ± 0.12	0.130	1.12	0.63	0.240	3.68 ± 0.06	0.37	1.13
4.9	2.83 ± 0.12	0.216	1.12	0.25	0.430	2.16 ± 0.06	0.75	1.08

the contribution of the shorter-lived component is seen to increase with concentration. Although this component has been attributed to dimer fluorescence [24] the absorption spectra show no evidence for H dimer formation, as would be indicated by a growth in the shoulder of the spectrum about 500 nm. Furthermore, these dimers are usually considered to have very low fluorescence yields. Other forms of dimer (oblique or J-type) have been reported for rhodamine 6G in sol–gel media [29], but the similarity between their spectrum and that of the monomer makes it difficult to obtain evidence of their presence. In any case these dimers would only be present in appreciable amounts for dye concentrations much higher than those used here. What appears clear is that the amount of the shorter-lived component is linked to a red shift in the emission maximum. Self-absorption effects, which could offer an explanation, are unlikely, as they should result in an increase in the mean decay time, which is contrary to what is observed. The decay time for rhodamine 6G in TEOS, with ethanol added to enhance solubility, was found to be 3.7 ns. This is a little higher than the values obtained for the shorter-lived component, but may hint, like the steady state fluorescence data that the dyes behaviour is influenced by the environment, e.g. an increasing amount becomes adsorbed to the silica displaying different photophysical parameters.

Narang et al. [24] have explained the time-resolved fluorescence behaviour by assuming that an efficient energy transfer from monomers to dimers takes place. An attempt was made to fit the data to a Förster model for energy transfer (Table 3) to ascertain if such kinetics could provide a better model for the data than that described in Table 2. Assuming a fluorescing monomer and non-fluorescent dimer it is found that except at the lowest concentration the gamma parameter increases with total concentration, but not as fast as would be expected for a monomer–dimer equilibrium. Other attempts (fixing the monomer lifetime at a constant value and having a second fluorescent species) yield no better fits to the data than those given in Table 2. We conclude that the most likely explanation is that fluorescence from dye molecules in different environments is being detected.

To see if any further information concerning the dyes environment could be elucidated a time-resolved anisotropy measurement was performed on the 0.24 mM sample. Due to the signal strength measurement of the lowest concentration sample was precluded. The raw data and the calculated anisotropy decay are presented in Fig. 3. The anisotropy decay shown in the figure still contains instrumental distortions and so the data was analysed using an impulse response reconvolution program (IBH Consultants). This yielded a value of 0.37 for the initial anisotropy (r_0), a rotational correlation time of 2.35 ± 0.66 ns and a limiting anisotropy (r_∞) of 0.238. The goodness of fit as reflected in the χ^2 value was 1.09. If the rotational time is used to provide an indication of the viscosity of the probes' environment then this can be calculated as 13.2 mPa s [30,31] [1]. A previous study probing a bulk TMOS matrix found the existence of two rotational

[1] Calculated using $\eta = (\tau_r kT)/V$, where V is the effective volume of the dye molecule (calculated using a radius of 5.6 Å), T the temperature and k the Boltzmann's constant.

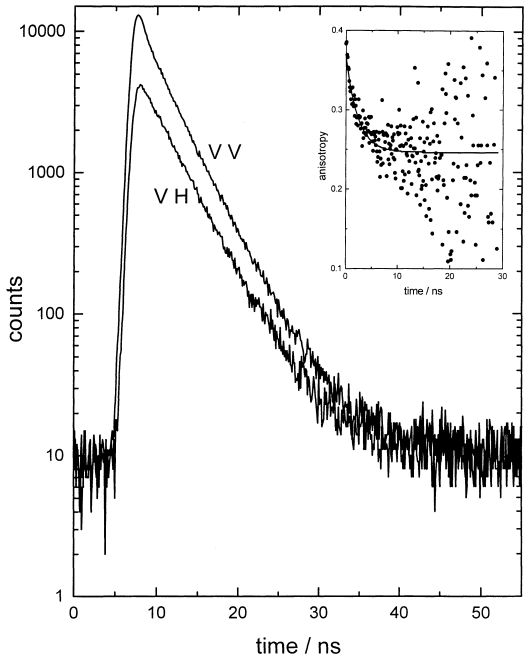

Fig. 3. Time-resolved anisotropy data for rhodamine 6G (ca. 0.24 mM) in a thin film matrix showing the vertical–vertical (VV) and vertical–horizontal (VH) polarisation data. The calculated anisotropy decay is presented in the inset. The time origin is arbitrary.

times, which were attributed to two pore environments of differing viscosity [23]. The large r_∞ value suggests a hindered rotation and is most likely because of dye adsorbed to the silica. In case this value was masking a longer rotational time, which is difficult to resolve because of the relatively short decay time of the probe, an attempt was made to fix r_∞ to zero and to analyse the data again adding a second rotational time. This form of analysis, however, did not produce any meaningful result. Again it appears most likely that the rhodamine 6G is reporting on different environments in the film matrix. One in which it could be partially solvated and able to rotate and another where it is adsorbed to the silica and any rotation is severely hindered. This observation is in agreement with our steady state and time-resolved data.

3.2.2. Bulk monoliths

As with the film samples different concentrations of rhodamine 6G were incorporated in the sol–gel monoliths. Due to the high concentrations used it was only possible to record the absorption spectra for the lower concentration samples (data not shown). As the film data suggests that there is a good correlation between the concentration of dye in the initial reaction mixture and that in the final 'dried' matrix we assume the same to be true for the bulk samples. This assumption appears to hold for the samples that we were able to measure and any indication of concentration is estimated on this basis. As with the film samples the spectra we were able to obtain did not provide evidence of aggregation effects.

The fluorescence spectra from these samples (measured in a right-angle geometry) are shown in Fig. 4. Here a pronounced red shift in the emission maximum can be seen. As there is an overlap between the absorption and emission bands in rhodamine 6G this behaviour is clearly indicative of self-absorption. Also this effect was found to be not as pronounced when the measurement geometry was changed to front face. Further evidence for self-absorption and secondary emission is seen in the time-resolved data (presented in Table 4). At the lowest concentration, unlike with the thin film samples, a monoexponential decay yielding a lifetime of 4.34 ns is obtained. However, on increasing the dye concentration there is a trend for the decay time to increase.

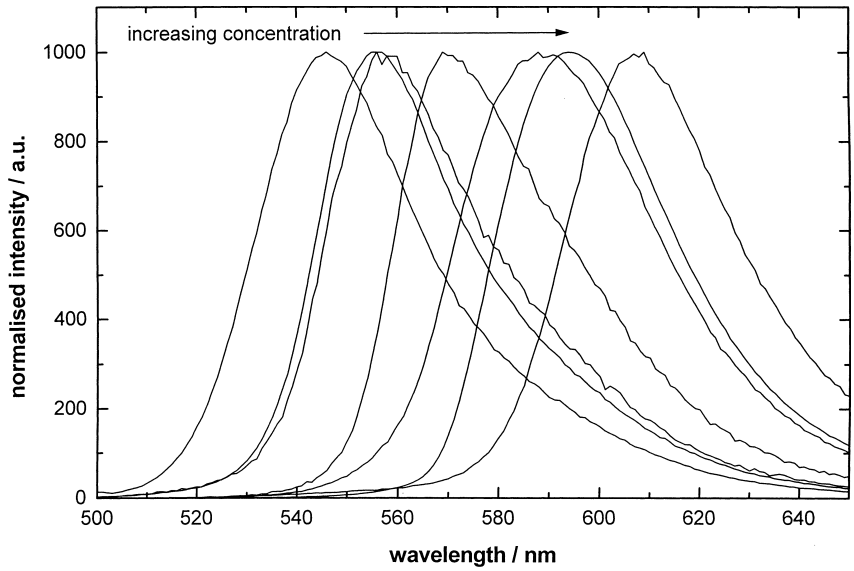

Fig. 4. Normalised steady state fluorescence spectra, recorded in 90° geometry, for various concentrations of rhodamine 6G in bulk samples. The excitation wavelength was 490 nm.

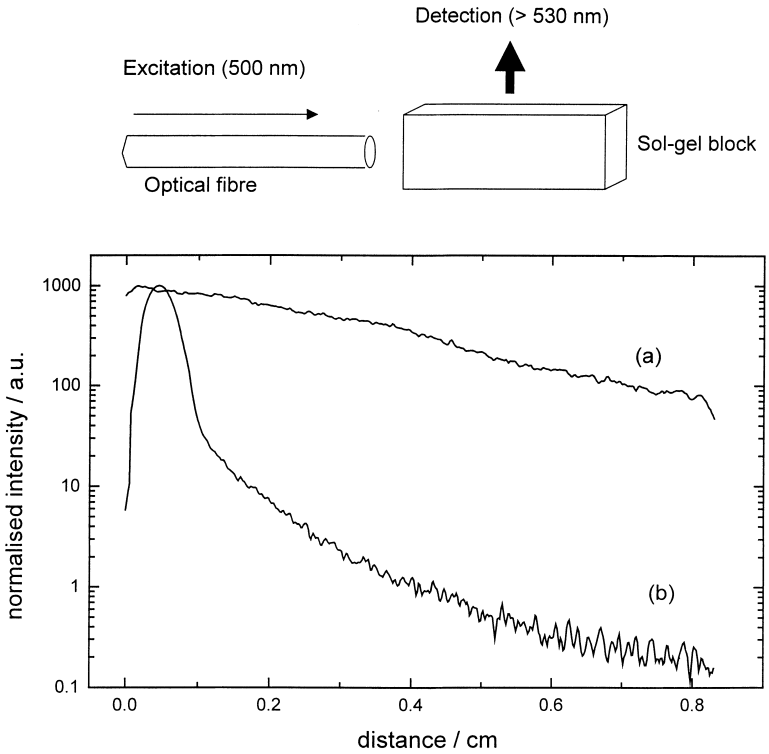

Fig. 5. Schematic representation for the observation of fluorescence intensity made using a photon counting fluorescence microscope. The intensity was monitored along the centre of the sample parallel to the excitation and 90°. (a) The response from a sol–gel derived bulk sample containing a dilute amount of rhodamine 6G. (b) The response obtained with a concentrated sample.

Table 4
Fluorescence decay time as a function of rhodamine 6G concentration in a bulk monolith. The negative sign in front of the pre-exponential factor indicates a 'rise-time'. '+' indicates concentration measured from the absorption spectrum, other values are estimates

Concentration (M)	Decay time (ns)	Pre-exponential	χ^2
4.0×10^{-6}+	4.34 ± 0.02		1.09
2.1×10^{-5}+	5.56 ± 0.02		1.13
2.1×10^{-4}	2.95 ± 0.84	−0.13	1.08
	6.18 ± 0.05	0.87	
1.2×10^{-3}	6.21 ± 0.03		1.12
2.0×10^{-3}	0.33 ± 0.24	−0.33	1.18
	6.37 ± 0.03	0.67	

Also some of the data requires the use of a second exponential containing a rise time (negative pre-exponential factor) to obtain a satisfactory fit. This is needed to fit the slightly convex shape of the fluorescence decay, which again is indicative of a self-absorption process occurring. It should also be noted that as the self-absorption effect appears to be the dominant process there is also the possibility that it may be masking other concentration effects like those seen in the thin film samples.

To assess the usefulness of this type of matrix to investigate the self-absorption phenomenon, the effect of distance from excitation source on the fluorescence intensity of the rhodamine 6G at both dilute and high concentrations when incorporated in the bulk matrix was observed. This was performed using a fluorescence microscope to observe the fluorescence and an optical fibre to channel the excitation light to the sample. The cone of light exiting the fibre had an angle of 57°. In order to quantify any self-absorption effect it is preferable to use parallel light, but the set up used serves well for a qualitative demonstration. This is represented in Fig. 6. For a low concentration of dye the behaviour is quite uniform with distance from the excitation source, curve (a). However, for the sample with the higher concentration of dye (b) this is clearly not the case. The behaviour that we observe is similar to that seen with a fibre-optic-based fluorimeter where inner-filter effects are observed [32]. The sol–gel glass provides an ideal matrix for studying this type of phenomenon as the matrix structure prevents collisional de-excitation of the fluorescent dyes within it. At this point of time it appears that the use of the sol–gel derived monolith shows promise in the study of self-absorption effects and we hope to provide a fuller treatment of this in the future (Fig. 5).

As with the film matrices a time-resolved anisotropy measurement was performed using the lowest concentration of dye to avoid any self-absorption effects. Fig. 6 shows the raw data along with the anisotropy decay. Again the data was analysed in the same way as with the films. However, in this case the use of a second rotational time and fixing r_∞ to zero seemed to provide the most meaningful result and provides a marginally better fit to the data. Justification for this also comes from the fact that the anisotropy decay still appears

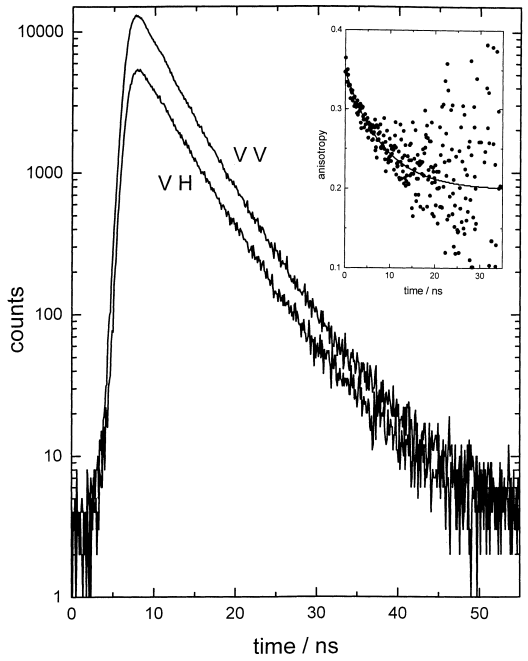

Fig. 6. Time-resolved anisotropy data for rhodamine 6G (ca. 4×10^{-6} M) in a bulk matrix showing the vertical–vertical (VV) and vertical–horizontal (VH) polarisation data. The calculated anisotropy decay is presented in the inset. The time origin is arbitrary.

to be decreasing with time (not the case with the film sample) and that this behaviour has previously been reported for TMOS derived matrices. [23]. The values recovered for the bulk matrix are $r_0 = 0.37$, a rotational time of 1.2 ± 1.5 ns (0.16) and a second rotational time of 34.6 ± 5.7 ns (0.84) with a χ^2 value of 1.12. The figures in parentheses represent the relative proportions. The goodness of the data is limited by the lifetime of the probe molecule on the longer timescale and by the resolution of our equipment in relation to the shorter times. If we use these rotational times to determine the viscosity then the values obtained are about 7 and 195 mPa s, respectively from the short and long rotational times. This suggests that the rhodamine 6G is located in solvent, which is not unreasonable as evidence exists for the presence of ethanol and water in this form of the matrix. However, even the lower viscosity value of 7 mPa s indicates that the solvent is more viscous than would be expected than if it had normal bulk properties. The second environment is an even more viscous one. This contrasts with the film sample in which most of the dye appears adsorbed and unable to rotate freely.

If one makes the analogy with inverse micelles to which the pore structure has been likened, especially if as in our case a majority of the pores in the bulk matrix are filled with liquid, then a rough estimate of pore size can be made from the viscosity data. This of course assumes that the viscosity is just affected by pore size and that the fluorophore is not adsorbed to the surface of the pore, which is filled with water and spherical in shape. Although not a rigorous treatment, using our viscosity values compared to those obtained for a AOT/trimethylpentane/water system [33] gives estimates for pore sizes of diameter about 2 nm (from the higher viscosity value) and over 20 nm (from the lower viscosity value). The former value, which would constitute the majority of the pores that we could probe in this manner, is close to that expected for silica sol–gel derived glasses [1,11]. In reality there is likely to be a distribution of sizes with the average size close to the lower value that we estimate.

3.3. Energy transfer between rhodamine 6G and malachite green

To further investigate the matrix we choose to perform a time-resolved fluorescence study using energy transfer between rhodamine 6G and malachite green. This was only attempted using the bulk samples, as a simple exponential decay of the donor was required to facilitate the analysis and the bulk samples were able to provide a better fluorescence signal. Energy transfer measurements have been previously used by Black and co-workers to monitor ageing in wet silica gels [27]. In all cases the data was analysed using a 3-D Förster model. A value for R_0 (the critical transfer distance) was first calculated and found to be about 43 Å [34] [2] from the overlap of the emission spectrum of rhodamine 6G and the absorption spectrum of malachite green measured at low concentration in sol–gel matrices. This is slightly lower than the value of 48 Å previously calculated for the system using glycerol [35].

The analysis of the decay data is presented in Fig. 7. The main part of this figure shows the change in the recovered gamma parameter with increasing acceptor (malachite green) concentration. In this case the concentration of rhodamine 6G in the stable bulk sample was determined as ca. 4×10^{-6} M from the absorption spectrum. In this analysis the recovered decay time appeared to remain reasonably constant, close to that obtained in the absence of malachite green, so collisional de-excitation is unlikely. An estimate for the diffusion length in ethanol gave a value of 24 Å, which is less than the R_0 value, substantiates this fact and the use of an energy transfer model. The analysis of the sample without any malachite green yielded an insignificant value of gamma, thus, negating donor–donor energy migration. Initially with small amounts of acceptor added there is a rather sharp increase in the gamma value, which then becomes less pronounced. Although the data can be fitted in the usual manner with a simple straight line (this gives an R_0 value of 91 Å), in this case it seems more appropriate to fit two regions separately. From the first region an R_0 of 104 Å is recovered and the other region yields a value of 67 Å for R_0. The first value is far greater than the calculated value of 43 Å, which indicates that the energy transfer process is a lot more efficient (ca. 200 times) than expected. The value of R_0 obtained from the second region is also larger than expected;

[2] Calculated using $R_0 = 9.79 \times 10^3 \ (\kappa^2 n^{-4} \Phi J)^{1/6}$ assuming $\kappa^2 = 2/3$, $\Phi = 0.95$, $n = 1.5$ and with $J = 6.02 \times 10^{-14}$.

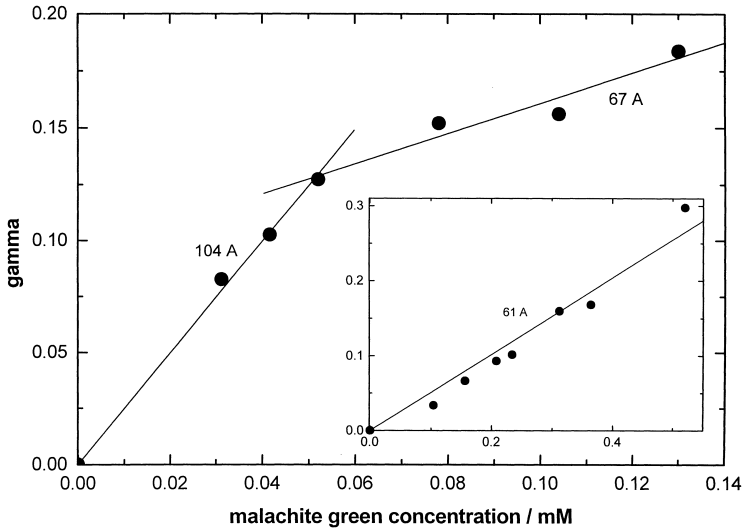

Fig. 7. Plot of gamma versus concentration of malachite green for a low concentration (4×10^{-6} M) of rhodamine 6G in a bulk matrix. The inset shows the behaviour for a higher concentration of rhodamine 6G (2.1×10^{-5} M).

here the efficiency is about 14 times higher. In order to further investigate this a larger concentration (2.1×10^{-5} M) of rhodamine was used (to produce a better fluorescence signal) along with correspondingly higher concentrations of malachite green. The variation of gamma with acceptor concentration is shown as an inset in Fig. 7. Here it seems realistic to fit the data to a linear regression. This yielded a value of 61 Å for R_0, which is close to that obtained in the second region in the main plot. This value is very similar to that obtained experimentally (62 Å) for this combination of dyes adsorbed to the surface of a vesicle [28].

These data are consistent with the matrix playing an important part in confining the dye molecules. The data can be interpreted in several ways and we assume that energy transfer does not occur between dye molecules located in different pores. It is possible to consider that there is a higher 'effective' acceptor concentration present, which gives rise to the larger R_0 values. Assuming that the value of 43 Å for R_0 is correct enables a comparison between the added acceptor concentration (obtained from the absorption spectra of the samples) and the effective acceptor concentration (calculated from the deviation of the data from the assumed R_0 value of 43 Å) to be made. This comparison (made for both datasets) is displayed in Fig. 8 and shows that for a small addition of acceptor molecules there is a sharp increase in the effective concentration. As both the donor and acceptor have comparable molecular structures it would be expected that their affinities for particular locations in the matrix should be similar. It could be that the observed behaviour can be explained by either the acceptor molecules initially taking up positions in more favourable environments, which happen to be close to the donors or there could be a distribution of pore sizes. Considering the former case the more favourable environments could include solvent filled pores or sites within the pores themselves, which

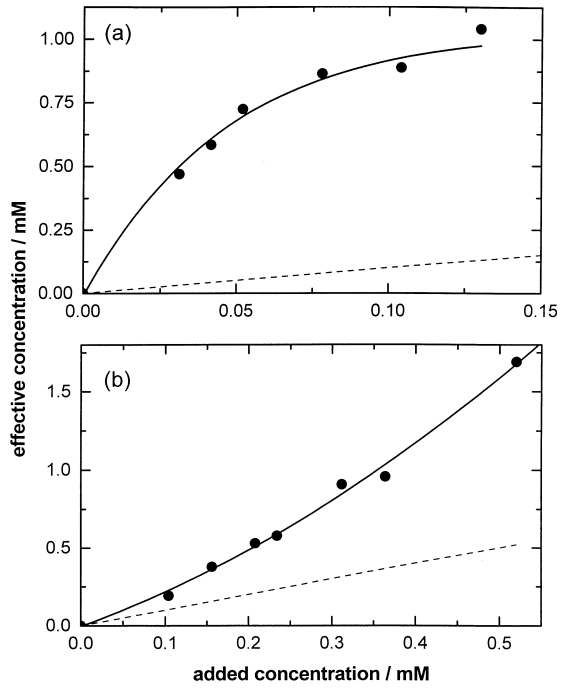

Fig. 8. Plot of the effective concentration of malachite green obtained from the R_0 values compared to that from the spectral data; (a) for the 4×10^{-6} M R6G concentration data, (b) the 2.1×10^{-5} M R6G concentration dataset. The dashed line represents 1 : 1 equivalence.

confine the donor and closer than would occur in an isotropic medium.

It is also likely that there is a distribution of pore sizes. The anisotropy data indicate that most will have a diameter in the order of 2 nm, although it also indicates the existence of pores with diameters 10 times larger. The ratio between theses two sizes is approximately 5.25 (0.84/0.16).

This corresponds well to the ratio obtained if we consider that the R_0 values for the lower and higher acceptor concentrations can be used to reflect pore volume [3] (i.e. $(104/61)^3$), which yields a ratio of 4.96. It is possible that energy transfer would be exhibited first in the smaller pores. Here the donor and acceptor could be held in close proximity (at a distance much less than the calculated R_0 value). This would produce very efficient energy transfer, while in larger pores the molecules have the ability to be situated farther apart, without affecting the enhanced energy transfer process to such an extent. As further dye molecules are added the main effect on the distribution of acceptor molecules comes from the large sized pores, although still their confinement of the molecules is such to lead to an enhancement of the efficiency of energy transfer in comparison to the calculated value.

4. Conclusion

From one sol–gel reaction mixture we are able to produce both thin film and bulk matrices, which are of good optical quality and appear stable in air. The work here suggests that the thin film samples are more porous than the bulk matrices. The latter are also found to contain a substantial amount of free liquid. Evidence for this comes from the NIR spectrum, DSC, TGA and the time-resolved anisotropy data. In the film samples it is unlikely that there is much free liquid although the anisotropy data suggests that some is present. The possibility exists that this may be bound water. Likening the pore structure to that of an inverse micelle allows for the estimation of pore size from the anisotropy data. This suggests that a majority of pores have a diameter in the order of 2 nm. On incorporation of the rhodamine into the two forms of matrix our results show no evidence of dye aggregation, although the energy transfer measurements imply that confinement by the pore structure can place molecules in relatively close proximity. It appears likely that the dye location in the bulk samples is mainly in solvated pores and a single decay time of 4.3 ns is obtained for a low concentration of encapsulated rhodamine 6G. In the thin film samples it appears that the dye is mainly adsorbed to the dry pore surface, which gives rise to a shorter-lived fluorescence component, with a small amount in solvated pores. This is observed from monitoring the change in the pre-exponential factors with increasing dye concentration. In the case of the bulk matrices any environmental effects are masked by the observation of self-absorption and secondary emission, which dominate the fluorescence behaviour of rhodamine 6G. This fact also demonstrates that the bulk matrix produced appears promising as a way to study this type of phenomenon.

[3] As the ratio of γ values for the low acceptor concentration ($R_0 = 104$ Å) region and higher concentration ($R_0 = 61$ Å) region ≡ ratio of effective concentrations (or effective volumes), i.e. $\gamma_{104}/\gamma_{61} = R^3{}_{0(104)}/R^3{}_{0(61)} = 4.95$.

Acknowledgements

Graham Hungerford would like to thank the Fundação para a Ciência e a Tecnologia (PRAXIS XXI) for financial support and the authors are grateful to Prof. M. Smith of the Dep. Química, Universidade do Minho for the DSC measurements.

References

[1] L.L. Hench, J.K. West, Chem. Rev. 90 (1990) 33.
[2] B. Dunn, J.I. Zink, J. Mater. Chem. 1 (1991) 903.
[3] D. Avnir, Acc. Chem. Res. 28 (1995) 328.
[4] R. Reisfeld, J. Non-Cryst. Solids 121 (1990) 254.
[5] V. Ramamurthy, Tetrahedron. 42 (1986) 5753.
[6] L.M. Ilharco, A.M. Santos, M.J. Silva, J.M.G. Martinho, Langmuir 11 (1995) 2419.
[7] H. Soyez, M. Huang, B. Dunn, J.I. Zink, Proc. SPIE 3136 (1997) 118.
[8] N. Negishi, T. Fujii, M. Anpo, HCR Concise Rev. 1 (1994) 231.
[9] Y. Takahashi, T. Kitamura, M. Nogami, K. Uchida, T. Yamanaka, J. Luminescence 60/61 (1994) 451.
[10] H. Nakazumi, T. Tarao, S.-I. Taniguchi, H. Nanto, Proc. SPIE 3136 (1997) 159.
[11] M. Casalboni, F. De Matteis, V. Ferone, P. Prosposito, R. Senesi, R. Pizzoferrato, A. Bianco, A. De Mico, Chem. Phys. Lett. 291 (1998) 167.
[12] S.K. Lam, D. Lo, Chem. Phys. Lett. 281 (1997) 35.
[13] D. Levy, D. Avnir, J. Photochem. Photobiol. A: Chem. 57 (1991) 41.
[14] K. Matsui, N. Usuki, Bull. Chem. Soc. Jpn. 63 (1990) 3516.
[15] P. Innocenzi, H. Kozaka, T. Yoko, J. Non-Cryst. Solids 201 (1996) 26.
[16] A. Dubois, M. Canva, A. Brun, F. Chapat, J.-P. Boilot, Appl. Optics 35 (1996) 3193.
[17] D. Avnir, D. Levy, R. Reisfeld, J. Phys. Chem. 88 (1984) 5956.
[18] L. Hu, Z. Jiang, Proc. SPIE 3136 (1997) 94.
[19] P. Boutin, J. Mugnier, B. Valeur, J. Fluorescence 7 (1997) 215S.
[20] K. Dou, X. Sun, X. Wang, E.K. Knobbe, Proc. SPIE 3136 (1997) 48.
[21] J.B. Birks, Photophysics of Aromatic Molecules, Wiley, New York, 1970.
[22] M.N. Berberan-Santos, E.J.N. Pereira, J.M.G. Martinho, in: D.L. Andrews, A.A. Demidov (Eds.), Resonance Energy Transfer, Wiley, New York, 1999, p. 108.
[23] U. Narang, R. Wang, P.N. Prasad, F.V. Bright, J. Phys. Chem. 98 (1994) 17.
[24] U. Narang, F.V. Bright, P.N. Prasad, Appl. Spectroscopy 47 (1993) 229.
[25] D. Oelkrug, W. Flemming, R. Füllemann, R. Günther, W. Honnen, G. Krabichler, M. Schäfer, S. Uhl, Pure Appl. Chem. 58 (1986) 1207.
[26] P. Innocenzi, H. Kozuka, T. Yoko, Phys. Chem. B 101 (1997) 2285.
[27] I. Black, D.J.S. Birch, D. Ward, M.J. Leach, J. Fluorescence 7 (1997) 111S.
[28] N. Tamai, T. Yamazaki, I. Yamazaki, A. Mizuma, N. Mataga, J. Phys. Chem. 91 (1987) 3503.
[29] T. Fujii, H. Nishikorori, T. Tamura, Chem. Phys. Lett. 233 (1995) 424.
[30] G. Porter, P.J. Sadkowski, C.J. Tredwell, Chem. Phys. Lett. 49 (1977) 416.
[31] U. Narang, R. Wang, P.N. Prasad, F.V. Bright, J. Phys. Chem. 98 (1994) 17.
[32] M.A. Victor, S.R. Croach, Appl. Spectroscopy 49 (1995) 1041.
[33] P.E. Zinsli, J. Phys. Chem. 83 (1979) 3223.
[34] R. Reisfeld, J. Non-Cryst. Solids 121 (1990) 254.
[35] D. Rehm, K.B. Eisenthal, Chem. Phys. Lett. 9 (1971) 387.